CHAPTER 13: ORGANOMETALLIC CHEMISTRY

13.1 Method A: = Donor-Pair Method, Method B: = Neutral-Ligand Method

a. $Fe(CO)_5$ A: $8 + 5 \times 2 = 18$ B: $8 + 5 \times 2 = 18$

b. $[Rh(bipy)_2Cl]^+$ A: $7 + 2 \times 4 + 2 = 17$ B: $9 + 2 \times 4 + 1 - 1 = 17$

c. $(\eta^5\text{-}Cp^*)Re(=O)_3$ A: $6 + 0 + 3 \times 4 = 18$ B: $5 + 7 + 3 \times 2 = 18$

d. $Re(PPh_3)_2Cl_2N$ A: $2 + 2 \times 2 + 2 \times 2 + 6 = 16$ B: $7 + 2 \times 2 + 2 \times 1 + 3 = 16$

e. $Os(CO)(\equiv CPh)(PPh_3)_2Cl$ A: $7 + 2 + 3 + 2 \times 2 + 2 = 18$ B: $8 + 2 + 3 + 2 \times 2 + 1 = 18$

f. $Ru(CE)Cl_2(NC_5H_4NMe_2)_2(C_3H_4N_2(C_8H_9)_2)$
A: $6 + 2 + 2 \times 2 + 2 \times 2 + 2 = 18$ B: $8 + 2 + 2 \times 1 + 2 \times 2 + 2 = 18$

13.2 All of these compounds have 16-electron valence configurations.

a. $Ir(CO)Cl(PPh_3)_2$ A: $8 + 2 + 2 + 2 \times 2 = 16$ B: $9 + 2 + 1 + 2 \times 2 =$
16

b. $RhCl(PPh_3)_3$ A: $8 + 2 + 3 \times 2 = 16$ B: $9 + 1 + 3 \times 2 = 16$

c. $[Ni(CN)_4]^{2-}$ A: $8 + 4 \times 2 = 16$ B: $10 + 4 \times 1 + 2 = 16$

d. *cis*-$PtCl_2(NH_3)_2$ A: $8 + 2 \times 2 + 2 \times 2 = 16$ B: $10 + 2 \times 2 + 2 \times 1 =$
16

13.3 **a.** $[M(CO)_7]^+$ A: $18 - 7 \times 2 = 4 = M^+$, **V** B: $18 - 7 \times 2 = 4 = M^+$, **V**

b. $H_3CM(CO)_5$ A: $18 - 2 - 5 \times 2 = 6 = M^+$, **Mn** B: $18 - 1 - 5 \times 2 = 7 = M$, **Mn**

c. $M(CO)_2(CS)(PPh_3)Br$ A: $18 - 2 \times 2 - 2 - 2 - 2 = 8 = M^+$, **Co**
B: $18 - 2 \times 2 - 2 - 2 - 1 = 9 = M$, **Co**

d. $[\eta^3\text{-}C_3H_3)(\eta^5\text{-}C_5H_5)M(CO)]^-$ A: $18 - 4 - 6 - 2 = 6 = M^+$, **Mn**
B: $18 - 3 - 5 - 2 = 8 = M^-$, **Mn**

e. $(OC)_5M{=}C(OCH_3)C_6H_5$ A and B: $18 - 5 \times 2 - 2 = 6 = M$, **Cr**

f. $[\eta^4\text{-}C_4H_4)(\eta^5\text{-}C_5H_5)M]^+$ A: $18 - 4 - 6 = 8 = M^{2+}$, **Ni** B: $18 - 4 - 5 = 9 = M^+$, **Ni**

g. $(\eta^3\text{-}C_3H_5)(\eta^5\text{-}C_5H_5)M(CH_3)(NO)$
A: $18 - 2 - 6 - 2 - 2 = 6 = M$, **Cr**
B: $18 - 3 - 5 - 1 - 3 = 6 = M$, **Cr**

h. $[\mathrm{M(CO)_4I(diphos)}]^-$ A: $18 - 4\times2 - 2 - 4 = 4 = \mathrm{M}$, **Ti**
B: $18 - 4\times2 - 1 - 4 = 5 = \mathrm{M}^-$, **Ti**

13.4 Calculating for each metal atom:

a. $[\mathrm{Fe(CO)_2(\eta^5\text{-}C_5H_5)}]_2$ A: $7 + 2\times2 + 6 = 17$, single Fe–Fe
B: $8 + 2\times2 + 5 = 17$, single Fe–Fe

b. $[\mathrm{Mo(CO)_2(\eta^5\text{-}Cp)}]_2^{2-}$ A: $5 + 2\times2 + 6 + 1 = 16$, double Mo=Mo
B: $6 + 2\times2 + 5 + 1 = 16$, double Mo=Mo

13.5 **a.** $[\mathrm{M(CO)_3(NO)}]^-$ linear M–N–O: A: $18 - 3\times2 - 2 - 2 = 8 = \mathrm{M}$, **Ru**
B: $18 - 3\times2 - 3 = 9 = \mathrm{M}^-$, **Ru**
bent M–N–O: A: $18 - 3\times2 - 2 = 10 = \mathrm{M}$, **Pd**
B: $18 - 3\times2 - 1 = 11 = \mathrm{M}^-$, **Pd**

b. $[\mathrm{M(PF_3)_2(NO)_2}]^+$ linear NO: A: $18 - 2\times2 - 2\times2 = 10 = \mathrm{M}^-$, **Rh**
B: $18 - 2\times2 - 2\times3 = 8 = \mathrm{M}^+$, **Rh**

c. $[\mathrm{M(CO)_4(\mu_2\text{–}H)}]_3$ As a triangular structure with three M–M bonds:
A: $18 - 4\times2 - 2 - 2 = 6 = \mathrm{M}^+$, **Tc**
B: $18 - 4\times2 - 1 - 2 = 7 = \mathrm{M}$, **Tc**

d. $\mathrm{M(CO)(PMe_3)_2Cl}$ A: $16 - 2 - 2\times2 - 2 = 8 = \mathrm{M}^+$, **Rh**
B: $16 - 2 - 2\times2 - 1 = 9 = \mathrm{M}$, **Rh**

13.6 Method B works better for calculating overall charge.

a. $[\mathrm{Co(CO)_3}]^z$ $9 + 3\times2 = 15$, $z = 3-$

b. $[\mathrm{Ni(CO)_3(NO)}]^z$ $10 + 3\times2 + 3 = 19$, $z = 1+$

c. $[\mathrm{Ru(CO)_4(GeMe_3)}]^z$ $8 + 4\times2 + 1 = 17$, $z = 1-$

d. $[\mathrm{(\eta^3\text{-}C_3H_5)V(CNCH_3)_5}]^z$ $3 + 5 + 5\times2 = 18$, $z = 0$

e. $[\mathrm{(\eta^5\text{-}C_5H_5)Fe(CO)_3}]^z$ $5 + 8 + 3\times2 = 19$, $z = 1+$

f. $[\mathrm{(\eta^5\text{-}C_5H_5)_3Ni_3(\mu_3\text{–}CO)_2}]^z$ $3\times5 + 3\times10 + 2\times2 = 49$, $z = 1+$, assuming three Ni–Ni bonds; calculating for each Ni: $5 + 10 + 2(2/3) + 2 = 18\ 1/3$; charge per Ni = 1/3+, overall charge = 1+
(Each triply bridging CO can be considered to donate 2 electrons overall, 2/3 electron to each metal.)

13.7 **a.** $[\mathrm{(\eta^5\text{-}C_5H_5)W(CO)}_x]_2$, assuming a single W–W: A: $6 + 5 + 1 + x\times2 = 18$, $x = 3$
B: $5 + 6 + 1 + x\times2 = 18$, $x = 3$

b. $\mathrm{ReBr(CO)}_x\mathrm{(CO_2C_2H_4)}$ A: $6 + 2 + x\times2 + 2 = 18$, $x = 4$
B: $7 + 1 + x\times2 + 2 = 18$, $x = 4$

c. $[\mathrm{(CO)_3Ni\text{–}Co(CO)_3}]^z$ A and B: $3\times2 + 10 + 2 + 9 + 3\times2 - z = 36$, $z = 3-$

d. $[\mathrm{Ni(NO)_3(SiMe_3)}]^z$ B: $10 + 3\times3 + 1 - z = 18$, $z = 2+$

e. $[(\eta^5\text{-}C_5H_5)Mn(CO)_x]_2$ B: $5 + 7 + 2 + x \times 2 = 18, x = 2$

13.8 **a.**

Upper ring: η^5-Cp	5 electrons
Co	9 electrons
	14 electrons; 4 more needed, so lower ring must be η^4

b.

M:	η^1-C_7 ring	1 electron	**M′**:	η^7-C_7 ring	7 electrons
	2 PEt_3	4 electrons		η^5-C_5 ring	5 electrons
	GeR_3	1 electron			12 electrons
		6 electrons		4 more needed to reach 16: Ti	

10 more needed to reach 16: Pt

13.9 Co (group 9):

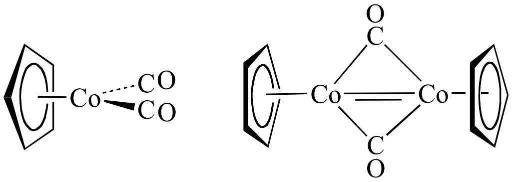

Ni (group 10):

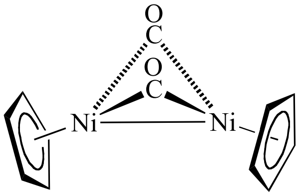

Cu (group 11):

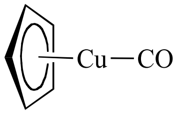

Other compounds with different hapticities for cyclopentadienyl ligands may also be possible.

13.10 Figure 10.19 gives an MO diagram for $Ni(CO)_4$ and cites additional references. The HOMOs (t_2) are strongly bonding, and there is a large energy gap between the HOMOs and the LUMOs in this 18-electron molecule.

13.11 The energy of stretching vibrations depends on the square root of the force constant divided by the reduced mass (Section 13.4.1).

The reduced masses are 14.73 for ^{16}O and 16.41 for ^{18}O, so $(14.73/16.41)^{1/2} = 0.947$, and the ^{18}O complex has vibrational energy of $0.947 \times 975\ cm^{-1} = 924\ cm^{-1}$. The value given in the reference is $926\ cm^{-1}$.

13.12 Sulfur is less electronegative than oxygen. Therefore, the tungsten in $W(S)Cl_2(CO)(PMePh_2)_2$ has greater electron density and a greater tendency to participate in π-backbonding with CO; a lower energy ν(CO) is expected (actual value: $1986\ cm^{-1}$).

13.13 Adding electrons to a carbonyl complex puts more electrons into the back-bonding t_{2g} orbitals. As a result, the V–C bonds in $[V(CO)_6]^-$ are strengthened and the distance shortened (but the C–O bonds are weakened by having more electrons in the t_{2g} orbitals, that are antibonding with respect to the C–O bonds.).

13.14 Sigma Donor Pi Acceptor

a.

b.

c.

13.15 **a.** If NO is counted as a linear donor, each of these has 18 electrons. The increasing nuclear charge (from formally Cr(0) to Mn(I) to Fe(II)) results in progressively less backbonding to the ligands and an increase in N–O bond order, leading to the higher NO stretching frequencies. The Cr species has an exceptionally low NO stretching frequency. It may have bent NO coordination, rendering it a 16 electron ion formally containing Cr(II). The Fe complex has a rather high NO stretching frequency, suggesting that π-backbonding is not a very large contribution to the electronic ground state of this complex.

b. The low energy band indicates bent NO coordination; the higher energy band is from the linear ligand. This complex has one of each, with angles of 138° and 178° (Greenwood and Earnshaw, *Chemistry of the Elements*, 2nd ed., pp. 450-52).

13.16 **a.** The CO_2 molecular orbitals are shown in Figure 5.25.

b. The π orbitals of 1,3,5-hexatriene are shown in Figure 13.21.

c. *cyclo*-C_4H_4:

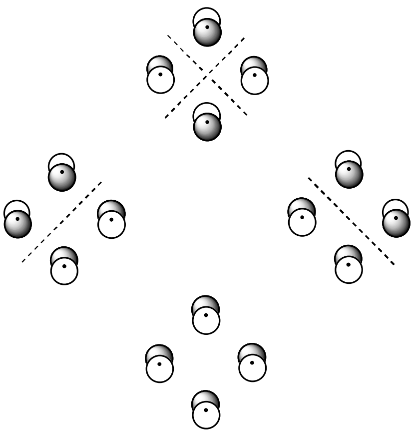

d. *cyclo*-C_7H_7:

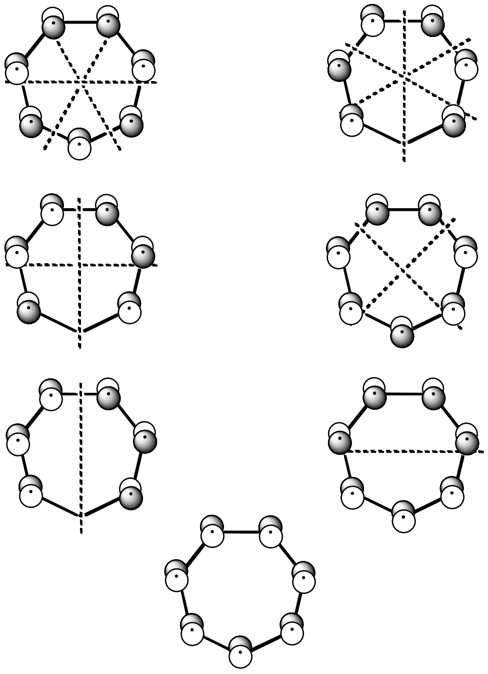

13.17 a. Using the group theoretical method described in Chapter 4: The four CO ligands are in a square planar arrangement, but the Mo atom is above them. The reducible representation Γ, shown below, can be derived for the C–O stretching vibrations. Γ reduces to $A_1 + B_1 + E$, with A_1 and E infrared active, so there are two bands visible (the E bands are degenerate).

C_{4v}	E	$2C_4$	C_2	$2\sigma_v$	$2\sigma_d$	
Γ	4	0	0	2	0	
A_1	1	1	1	1	1	z
B_1	1	–1	1	1	–1	
E	2	0	–2	0	0	(x, y)

b.

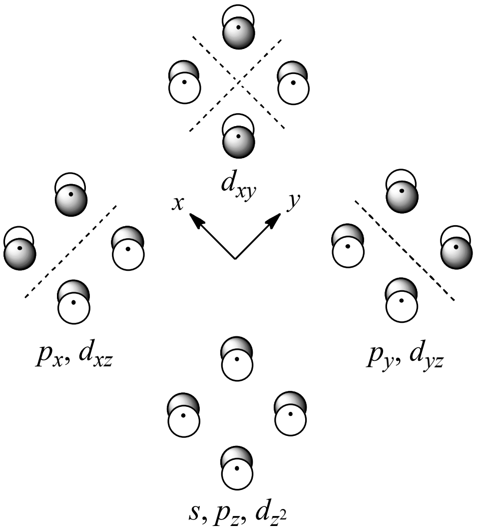

13.18 **a.** From bottom to top:

0-node, left, is A_1', 0 node, right is A_2''
1-node, far left and third from left are E_1'
1-node, second from left and far right are E_1''
2-node, far left and third far left are E_2'
2-node, second from left and far right are E_2''

b.

s, d_{z^2}	(d_{xy}, $d_{x^2-y^2}$)	(d_{xy}, d_{yz})	p_z	(p_x, p_y)
A_1'	E_2'	E_1''	A_2''	E_1'

c. The matching orbitals are shown in part b; there is no match in the Fe orbitals for the E_2'' ligand orbitals.

13.19 **a.** The π orbitals of benzene are shown in Figure 13.22.

b. Group orbitals

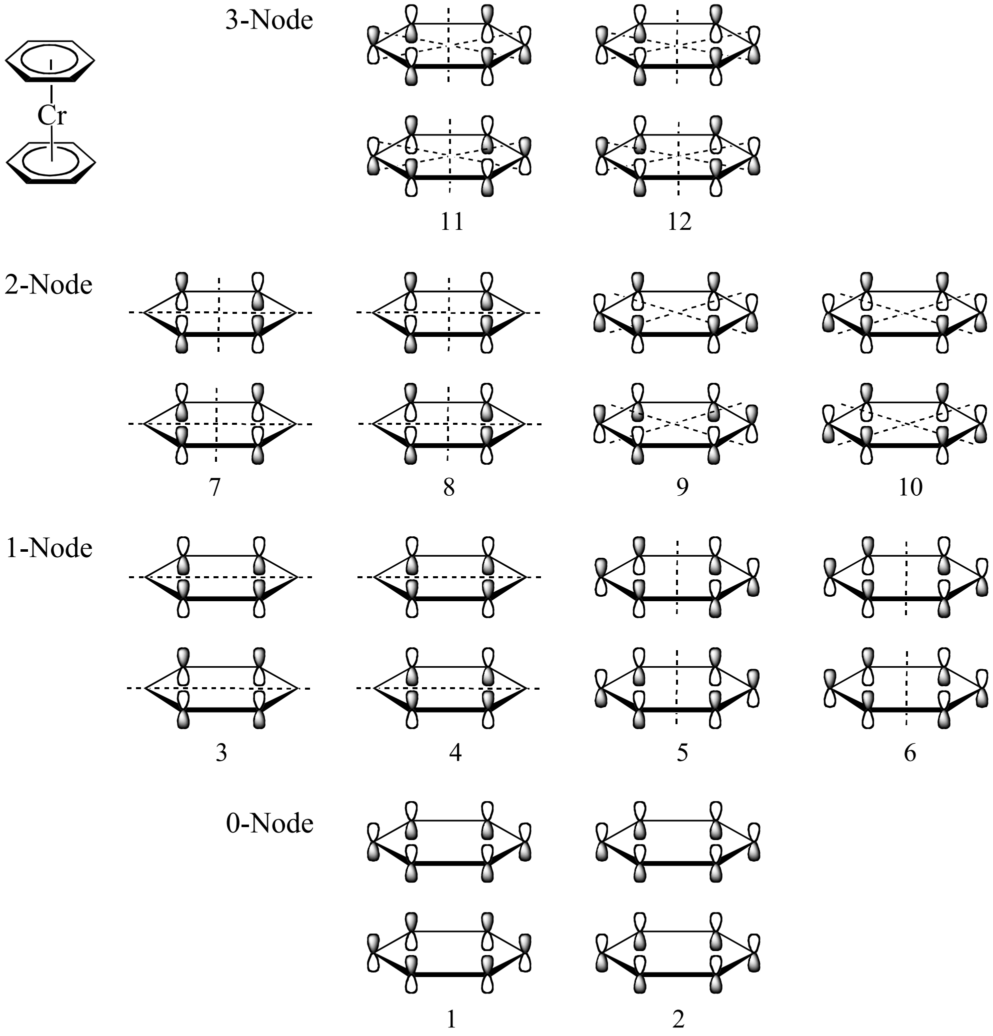

c. Matching Cr orbitals:

1	s, d_{z^2}	7	d_{xy}
2	p_z	8	none
3	p_y	9	$d_{x^2-y^2}$
4	d_{yz}	10	none
5	p_x	11	none
6	d_{xz}	12	none

d. Energy level diagram

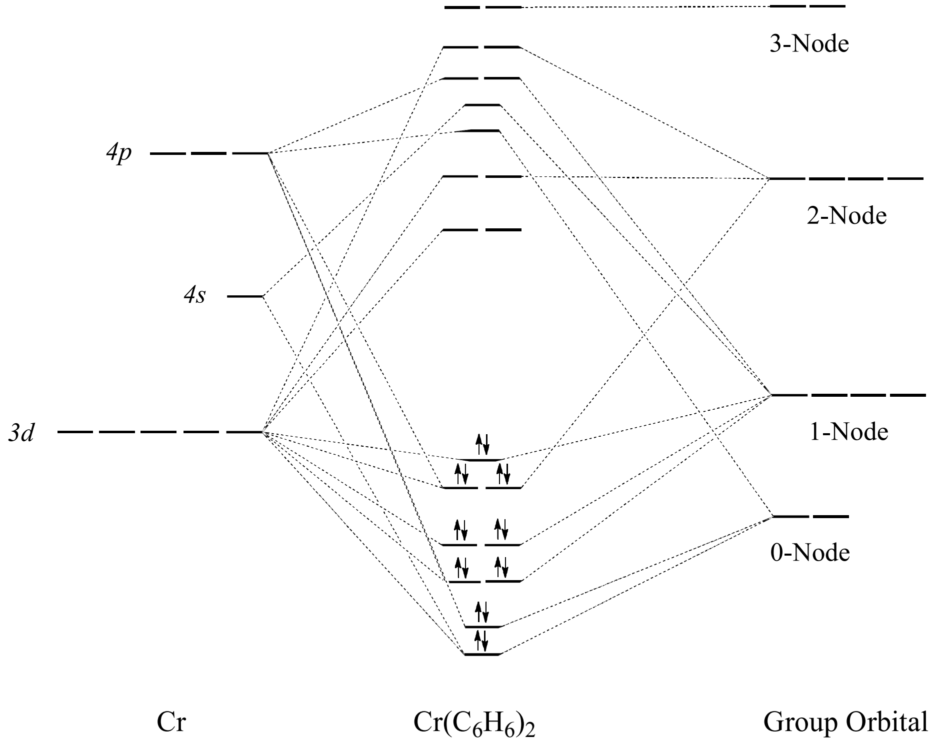

13.20 **a.** Point group: C_{2v} (in orientation shown)

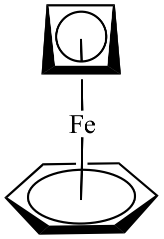

b. The reducible representation is Γ:

C_{2v}	E	C_2	$\sigma_v\ (xz)$	$\sigma_v'\ (yz)$		
Γ	10	0	2	0		
A_1	1	1	1	1	z	x^2, y^2, z^2
A_2	1	1	−1	−1		xy
B_1	1	−1	1	−1	x	xz
B_2	1	−1	−1	1	y	yz

c. $\Gamma = 3A_1 + 2A_2 + 3B_1 + 2B_2$

Representations	Matching orbitals of Fe
A_1	s, p_z, d_{z^2}
A_2	d_{xy}
B_1	p_x, d_{xz}
B_2	p_y, d_{yz}

13.21

C_{3v}	E	$2C_3$	$3\sigma_v$	
Γ	3	0	1	
A_1	1	1	1	z
A_2	1	1	–1	
E	2	–1	0	(x, y)

$\Gamma = A_1 + E$, both IR active. There are three vibrations, but two are degenerate, so two C–O stretching bands are expected in the IR spectrum.

13.22 $Ni(CO)_4$

T_d	E	$8C_3$	$3C_2$	$6S_4$	$6\sigma_d$	
Γ	4	1	0	0	2	
A_1	1	1	1	1	1	
T_2	3	0	–1	–1	1	(x, y, z)

$\Gamma = A_1 + T_2$ A_1 is IR inactive, T_2 is IR active: 1 band.

$Cr(CO)_6$

O_h	E	$8C_3$	$6C_2$	$6C_4$	$3C_2$	i	$6S_4$	$8S_6$	$3\sigma_h$	$6\sigma_d$	
Γ	6	0	0	2	2	0	0	0	4	2	
A_{1g}	1	1	1	1	1	1	1	1	1	1	
E_g	2	–1	0	0	2	2	0	–1	2	0	
T_{1u}	3	0	–1	1	–1	–3	–1	0	1	1	(x, y, z)

$\Gamma = A_{1g} + E_g + T_{1u}$ Only T_{1u} is IR active: 1 band

13.23

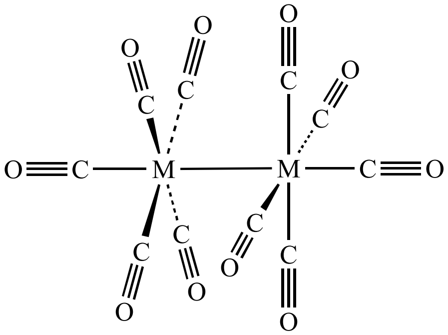

D_{4d}	E	$2S_8$	$2C_4$	$2S_8^3$	C_2	$4C_2'$	$4\sigma_d$	
Γ	10	0	2	0	2	0	4	
A_1	1	1	1	1	1	1	1	
B_2	1	–1	1	–1	1	–1	1	z
E_1	2	$\sqrt{2}$	0	$-\sqrt{2}$	–2	0	0	(x, y)
E_2	2	0	–2	0	2	0	0	
E_3	2	$-\sqrt{2}$	0	$\sqrt{2}$	–2	0	0	(R_x, R_y)

$\Gamma = 2A_1 + 2B_2 + E_1 + E_2 + E_3$ $\quad$ $2B_2$ and E_1 are IR active: 3 bands

13.24 a.

$W(CO)_5(NCC_3H_7)$	2077, 1975, 1938 cm^{-1}
$W(CO)_4(NCC_3H_7)_2$, *cis*	2107, 1898, 1842 cm^{-1}
$W(CO)_3(NCC_3H_7)_3$, probably *fac*	1910, 1792 cm^{-1}

Pentacarbonyls have three active IR stretches, tetracarbonyls have one (other ligands *trans*) or four (other ligands *cis*), and tricarbonyls have two (*fac*) or three (*mer*) (see Table 13.10). It appears that two of the tetracarbonyl bands have similar enough energies for their bands to overlap, so only three appear in the spectrum (or one band may be so weak in intensity that it does not appear), but that the nitriles must be *cis*. The evidence for the *fac* isomer of the tricarbonyl is not conclusive based on the IR spectrum alone, since again two bands of the *mer* isomer might overlap.

b. The stretching energy of the CO *trans* to the nitrile ligand is lower than that for CO *cis* due to reduced competition for the π backbonding electrons (CO is a better π-acceptor). In the second complex, two are *cis* and two are *trans*. In the third complex, all three are *trans*, so the band energy is lower. In general, the trend is to lower energies as CO is replaced by butyronitrile; butyronitrile is not as effective a π acceptor as CO, so the π-acceptor nature of CO is enhanced as more nitrile ligands are added.

c. As more CO ligands are replaced by nitriles, which are stronger at donating electrons to Mo, the remaining CO ligands become stronger π acceptors, and the Mo–C bonds become stronger. In $Mo(CO)_3(NCC_3H_7)_3$ the Mo–C bond is so strong that the complex cannot react further with butyronitrile.

13.25 a. The bands at lower energy are for the CO ligands. The C–O stretches, which involve a greater change in dipole moment, are more intense than the C–N stretches. Because CO has a slightly greater reduced mass than CN, C–O stretches should occur at lower energies than C–N stretches; the energy of vibrational levels is inversely proportional to

$\sqrt{\text{reduced mass}}$. Also, the greater π-acceptor ability of the CO ligand is a contributing factor to the lower energy stretches for this ligand.

b. The *trans*-$[Fe(CO)_2(CN)_4]^{2-}$ complex should have a single IR-active C–O stretch (only the antisymmetric stretch is IR active) and a single IR-active C–N stretch (see Table 13.7). The *cis* complex should have two IR-active C–O stretches (both symmetric and antisymmetric) and four IR-active C–N stretches. In addition to its single carbonyl stretch, $[Fe(CO)(CN)_5]^{3-}$ would be expected to have three IR-active C–N stretches. The correct identifications are therefore:

	Predicted on basis of symmetry	
Complex	C–O stretches	C–N stretches
A: *cis*-$[Fe(CO)_2(CN)_4]^{2-}$	2	4
B: *trans*-$[Fe(CO)_2(CN)_4]^{2-}$	1	1
C: $[Fe(CO)(CN)_5]^{3-}$	1	3

In complexes **A** and **C**, some of the C–N stretches are too weak to be seen or the bands overlap; otherwise, the expected numbers of bands and the observed spectra match.

13.26 **a.** The CO ligand can be in either the axial or the equatorial position on the trigonal bipyramidal complex. These environments are not equivalent, so the two isomers should have different carbonyl stretching bands.

b. The CO stretch absorbs at a higher energy in $Fe(CO)(PF_3)_4$, implying that the C–O bond is stronger in that compound. If the CO bond is stronger, the Fe–C bond is correspondingly weaker, indicating that the PF_3 ligands are better π acceptors and therefore higher in the spectrochemical series than CO.

13.27

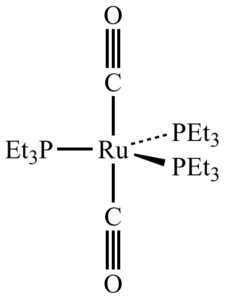

One C–O stretch (antisymmetric) (minor isomer)

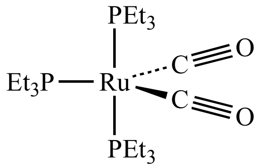

Two C–O stretches (symmetric and antisymmetric) (major isomer)

13.28 From Table 13.10, $[Co(CO)_3(PPh_3)_2]^+$ must be trigonal bipyramidal with all three CO ligands in the equatorial plane, giving rise to a single C–O absorption band.

13.29 By extrapolation of the positions of the C–O bands for $[Mn(CO)_6]^+$ (2100 cm^{-1}) and $[Fe(CO)_6]^{2+}$ (2204 cm^{-1}), one might predict a comparable band for $[Ir(CO)_6]^{3+}$ near 2300 cm^{-1}. Actual value: 2254 cm^{-1}.

13.30 **a.** In these three cations, the high metal oxidation states significantly reduce backbonding.

This effect is greatest for $[Hg(CO)_2]^{2+}$, with a charge of 1+ per CO, and weakest for $[Os(CO)_6]^{2+}$, with a charge of 1/3+ per CO. Therefore, $[Os(CO)_6]^{2+}$ should have the strongest backbonding, weakest C–O bond, and lowest energy carbon-oxygen stretching vibration. The actual energies are listed on the next page.

	$\nu(CO)$, cm^{-1}
$[Hg(CO)_2]^{2+}$	2278
$[Pt(CO)_4]^{2+}$	2244
$[Os(CO)_6]^{2+}$	2190

b. A reducible representation for this ion based on C–O stretching vibrations would have the following characters:

D_{2d}	E	$2S_4$	C_2	$2C_2'$	$2\sigma_d$	
Γ	6	0	2	0	4	
$2A_1$	2	2	2	2	2	
$2B_2$	2	–2	2	–2	2	z
E	2	0	–2	0	0	(x, y)

There should be three carbon–oxygen stretching bands, two of B_2 symmetry and one of E symmetry (a degenerate pair). With a charge 2+, this complex should exhibit infrared bands near those of $[Fe(CO)_6]^{2+}$ (2204 cm^{-1}). Actual bands are observed at 2173 cm^{-1} (E) and at 2187 and 2218 cm^{-1} (B_2).

13.31 a. The representation based on the set of six C–O vibrations in O_h symmetry is:

O_h	E	$8C_3$	$6C_2$	$6C_4$	$3C_2(=C_4^2)$	I	$6S_4$	$8S_6$	$3\sigma_h$	$6\sigma_d$
Γ	6	0	0	2	2	0	0	0	4	2

This representation reduces to $A_{1g} + E_g + T_{1u}$ (see Exercise 10.4). Of these, A_{1g} and E_g match squared functions and are therefore Raman active. (A_{1g} matches the band at 2015 cm^{-1} and E_g matches the band at 2119 cm^{-1}.)

b. **J**, **K**, and **L** are, respectively, the products of substitution of CO by py: $Mo(CO)_5py$, *cis*-$Mo(CO)_4py_2$, and *fac*-$Mo(CO)_3py_3$. As the number of pyridine ligands increases, the strong σ donation by this ligand increases the backbonding by the CO ligands, resulting in successive lowering in energy of the C–O vibrations. Symmetry analysis of each of these complexes shows more expected Raman-active bands than reported in the article. Additional weak bands can be seen in the Raman spectra (shown in the reference).

13.32 $(\eta^5\text{-}C_5H_5)Cr(CO)_2(NS)$ 1962, 2033 cm^{-1}

$(\eta^5\text{-}C_5H_5)Cr(CO)_2(NO)$ 1955, 2028 cm^{-1}

NS is a stronger π acceptor, so the CO backbonding is reduced in $(\eta^5\text{-}C_5H_5)Cr(CO)_2(NS)$ and the C≡O bond is strengthened and has a higher stretching energy.

13.33 The energy for a stretching vibration is proportional to $\sqrt{\frac{k}{\mu}}$, where k is the force constant and μ is the reduced mass (Section 13.4.1). In this case, the reduced masses for the N–S stretches are: ^{14}N–S: $\mu = \dfrac{14.00 \times 32.06}{14.00 + 32.06} = 9.745$ ^{15}N–S: $\mu = \dfrac{15.00 \times 32.06}{15.00 + 32.06} = 10.22$.

Because the energy is inversely proportional to the square root of the reduced mass, we can write:

$$\frac{E(^{15}\text{N–S})}{E(^{14}\text{N–S})} = \sqrt{\frac{\mu(^{14}\text{NS})}{\mu(^{15}\text{NS})}} = \sqrt{\frac{9.745}{10.22}} = 0.9765$$ The expected position of the N–S stretch in the ^{15}NS complex is therefore 0.9765 × 1284 cm^{-1} = 1254 cm^{-1}. The reported value is 1248 cm^{-1}.

13.34 Because the reduced mass of ^{13}CO is greater than the reduced mass of ^{12}CO, the separation between vibrational energy levels should be less for ^{13}CO, and the ^{13}CO complex should therefore show an infrared band at lower energy than 2199 cm^{-1}. Actual value: 2149 cm^{-1}.

13.35 **a.** $Mo(CO)_6 + Ph_2PCH_2PPh_2 \longrightarrow$ 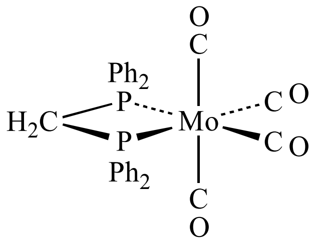 + 2 CO

b. $(\eta^5\text{-}C_5H_5)(\eta^1\text{-}C_3H_5)Fe(CO)_2 \xrightarrow{h\nu} (\eta^5\text{-}C_5H_5)(\eta^3\text{-}C_3H_5)Fe(CO) + CO$

The allyl ligand can bond in either η^1 or η^3 fashion. Loss of CO converts the reactant from 18 electrons to 16 electrons; rearrangement of allyl from η^1 to η^3 returns it to 18 electrons.

c. $(\eta^5\text{-}C_5Me_5)Rh(CO)_2 \longrightarrow [(\eta^5\text{-}C_5Me_5)Rh(CO)]_2 + 2\ CO$

A double Rh–Rh bond is needed; CO ligands may be bridging or terminal (the electron count is the same for both modes).

d. $V(CO)_6 + NO \longrightarrow V(CO)_5(NO) + CO$

The compound changes from 17 to 18 electrons.

e. $W(CO)_5{=}C(C_6H_5)(OC_2H_5) + BF_3 \longrightarrow [(CO)_5W{\equiv}CC_6H_5]^+ + F^- + F_2BOC_2H_5$

f. $[(\eta^5\text{-}C_5H_5)Fe(CO)_2]_2 + 2\ Al(C_2H_5)_3 \longrightarrow$

(See Figure 13.17)

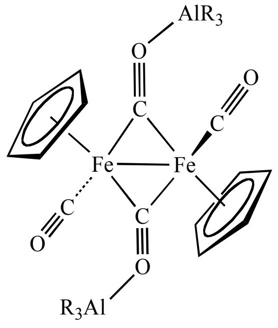

13.36	ν(CO), cm^{-1}
$P(t\text{-}C_4H_9)_3$	1923 (best σ donor, poorest π acceptor)

$P(p\text{-}C_6H_4Me)_3$	1965
$P(p\text{-}C_6H_4F)_3$	1984
$P(C_6F_5)_3$	2004 (best π acceptor)

13.37 **a.** $Fe(CO)_4(PF_3)$ (PF_3 is a strong π acceptor)

b. $[Re(CO)_6]^+$

c. $Mo(CO)_3(PCl_3)_3$ (PCl_3 is the best π acceptor among the phosphines)

13.38 **a.** Oxidation of these low-spin d^6 octahedral complexes causes loss of 1 t_{2g} electron, resulting in a change in LFSE of 0.4 Δ_o (from $-2.4\ \Delta_o$ to $-2.0\ \Delta_o$).

b. The C—O distance decreases. As the oxidation state of Cr increases from 0 to 1+, the CO ligands become weaker pi acceptors, and there is less occupation of π* orbitals in the ligands; consequently, the bonding in these ligands is stronger in the cations than in the neutral complexes (in the reference, the calculated decrease in C—O distances is in the range of 0.015 - 0.020 Å).

c. The Cr—P distance increases (calculated increase: 0.094Å) as the phosphine ligand becomes a weaker pi acceptor; there is less backbonding in the cation than in the neutral complex.

d. The Cr—N distance decreases.

13.39 In order from highest to lowest ν:

$Mo(CO)_4\,(F_2PCH_2CH_2PF_2)$	has strongest acceptor diphosphine
$Mo(CO)_4\,((C_2F_5)_2PCH_2CH_2P(C_2F_5)_2)$	
$Mo(CO)_4\,((C_6F_5)_2PCH_2CH_2P(C_6F_5)_2)$	
$Mo(CO)_4\,(Ph_2PCH_2CH_2PPh_2)$	
$Mo(CO)_4\,(Et_2PCH_2CH_2PEt_2)$	has strongest donor diphosphine

13.40 Coordinated N_2 has a lower stretching energy than free N_2. N_2 can act as a π acceptor, weakening the N–N bond and lowering the energy of the stretching vibration. The stretching vibration of free N_2 is IR inactive; there is no change in dipole moment on stretching.

13.41 At the higher temperature, the $-O-CH_3$ group should rotate rapidly enough to show only a single, average environment, so each CH_3 has a single peak. At low temperatures, this rotation can be restricted, and *cis* and *trans* isomers result (see Figure 13.45). The larger peaks represent the more prevalent isomer.

13.42 At high temperature, the C_5H_5 rings undergo rapid 1,2 shifts to give a single average proton signal on the NMR time scale. At sufficiently low temperature, the different environments of the η^1 and η^5 rings can be seen. The relative intensities are a = 1, b = 2, c = 2, and d = 5.

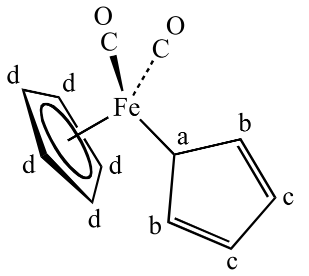

13.43 PF_3 is a stronger π acceptor than PCl_3. As a result, the chromium in $Cr(CO)_5(PCl_3)$ has a greater electron density, and CO acts as a stronger π acceptor in this complex. As a result:

a. $Cr(CO)_5(PF_3)$ has the stronger and shorter C–O bonds.

b. $Cr(CO)_5(PCl_3)$ has the higher energy Cr–C bands; since CO acts as a better π acceptor in this complex, the Cr–C bond is strengthened.

13.44 a. $[Fe(NO)(mnt)_2]^-$ has less electron density on Fe, less backbonding to NO, and a stronger N–O bond with higher stretching frequency.

b. $(CO)_5Cr{:}N{\equiv}N{:}Cr(CO)_5$ N_2 acts as a π acceptor toward both metals, significantly weakening the N–N bond.

c. $Ta{=}CH_2$ has a shorter Ta–C bond because it is a double bond.

d. $Cr{\equiv}CCH_3$ has a triple bond, which is shorter than either of the Cr–C bonds to CO ligands.

e. $[Fe(CO)_4]^{2-}$ has more π backbonding because Fe has the lowest nuclear charge of the metals in this isoelectronic series; this reduces the C≡O bonding and the energy of the C–O vibration.

13.45 Figure 13.51 shows the highest occupied orbital in the four-atom pi system of the ruthenium analogue to the dimanganese complexes in this problem. This orbital, with two nodes between the metals, is shown below.

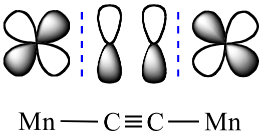

A similar orbital is involved in the dimanganese complexes. Oxidation of the neutral complex, by removing electrons from this orbital, should weaken and lengthen the carbon–carbon bond (removing electrons from an orbital that is C–C bonding) and strengthen and shorten the manganese–carbon bonds (removing electrons from an orbital that is Mn–C antibonding).

13.46 a. MX_6

b. $ML_4X_5^+ \longrightarrow ML_3X_6$

c. $ML_4^{2-} \longrightarrow ML_4X_2$

d. ML_5X_2

e. ML_4X_2

f. $ML_4X_2^+ \longrightarrow ML_3X_3$

13.47 a. $ML_3X_3^{3+} \longrightarrow MX_6$

$[FeCl_3(PPh_3)_3]^{3+}$ belongs to an unknown class of iron complexes, and this cation has not been reported.

b. $ML_2X_3^+ \longrightarrow MX_4L$

$[FeCl_3(PPh_3)_2]^+$ belongs to an unknown class of iron complexes, and this cation has not been reported.

c. $MX_2L_2^+ \longrightarrow MX_3L$

$[FeCl_2(PPh_3)_2]^+$ belongs to an unknown class of iron complexes, and this cation has not been reported.

d. MX_2L_2

$FeCl_2(PPh_3)_2$ is a member of a class with less than 1% of known Fe complexes. The crystal structure of $FeCl_2(PPh_3)_2$ was reported in 2005 (O. Seewald, U. Flörke, G. Henkel, *Acta Cryst.*, **2005**, *E61*, m1829).

13.48 One CO is replaced by 2-butyne. The NMR peaks are due to ethyl CH_3 ($\delta = 0.90$), ethyl CH_2 ($\delta = 1.63$), and butyne CH_3 ($\delta = 3.16$). The $\delta = 3.16$ peak splits at low temperatures because the two ends of the butyne are not identical; at higher temperatures, they become identical on NMR time scale, perhaps through rotation about the Mo–butyne bond. The single ^{31}P peak indicates identical PEt_3 groups, suggesting the isomer shown. The IR indicates that a CO ligand remains on the compound; the molecular weight of the compound shown is 574.2, well within the limits given.

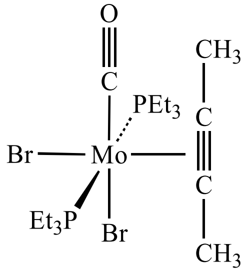

13.49 The analysis fits $[(\eta^5\text{-}C_5H_5)Fe(\mu\text{–}CO)_3Fe(\eta^5\text{-}C_5H_5)]$. The single CO band is consistent with this structure. Using D_{3h} symmetry for the central part of the molecule, a representation based on the bridging carbonyls reduces to A_1' (IR-inactive) plus E' (IR-active); the observed absorption is for the E' vibration.

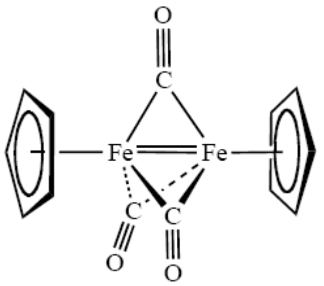

D_{3h}	E	$2C_3$	$3C_2$	σ_h	$2S_3$	$3\sigma_v$	
Γ	3	0	1	3	0	1	
A_1'	1	1	1	1	1	1	
E'	2	–1	0	2	–1	0	(x, y)

13.50 $(\eta^5\text{-}C_5H_5)$ $(\eta^3\text{-}C_5H_7)Ni$ There are 5 η^5 protons, 4 on the two carbons of the second Cp ring that are not bonded to Ni, 2 on the first and third carbons bonded to Ni, and 1 on the center C bonded to Ni.

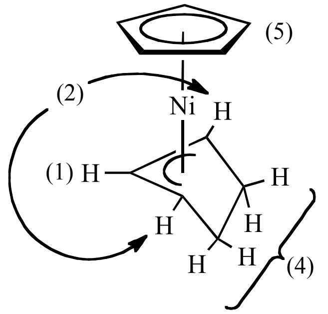

13.51 $I_s/I_a = \cot^2(\phi/2) = \cot^2 38° = 1.64$

13.52 **a.** In the $\eta^6\text{-}C_6H_6$ complex, CO is acting as a stronger π acceptor, as shown in its lower energy C–O stretching vibrations. Because the concentration of electrons on Cr is therefore greater in the η^6-C_6H_6 complex, η^6-C_6H_6 is donating more strongly to Cr than is the η^6-C_4BNH_6 ligand, so η^6-C_4BNH_6 is the stronger acceptor.

b. The longest C–C distance is the bond opposite the B–N bond, as in the resonance structure shown. The nitrogen attracts electrons from its neighboring carbon, which in turn attracts electrons from the next carbon, enhancing the bond strength between these two carbons and resulting in the shortest C–C bond, 1.374 Å. In the π orbitals (see Figure 13.22 for benzene), one of the occupied π orbitals is antibonding with respect to the C–C bond opposite the B–N bond, consistent with this C–C bond being the longest in the molecule.

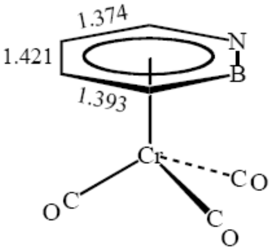

13.53 **a.** Mass of C_{60}:

C_{60}:	720	
Ir:	193	(most abundant isotope)
CO:	28	
C_9H_7:	115	
	1056	

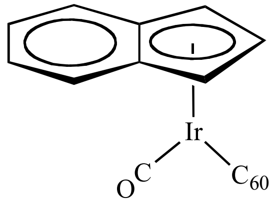

b. Because the carbonyl stretch decreases by 44 cm^{-1}, there must be a significant decrease in the electron density at Ir.

c. The C_{60} is replaced by PPh_3, giving $(\eta^5\text{-}C_9H_7)Ir(CO)(PPh_3)$.

13.54

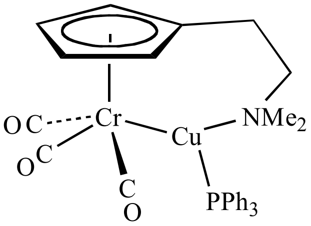

Spectral data are interpreted in the reference.

13.55 If CO is liberated from $(\eta^5\text{-}C_5H_5)Mn(CO)_3$, it must be replaced by some other ligand if the 18-electron rule is to be maintained. In this case, the new ligand is tetrahydrofuran (THF), a cyclic ether that can act as a sigma donor, and compound **Q** is $(\eta^5\text{-}C_5H_5)Mn(CO)_2(THF)$:

$$(\eta^5\text{-}C_5H_5)Mn(CO)_3 + THF \longrightarrow \underset{\mathbf{Q}}{(\eta^5\text{-}C_5H_5)Mn(CO)_2(THF)} + CO$$

The NC groups on carbon in $H_2C(NC)_2$ can act as donors to transition metals; each has a lone pair on carbon. In the formation of **R**, the weakly bound THF is replaced by a $H_2C(NC)_2$ ligand:

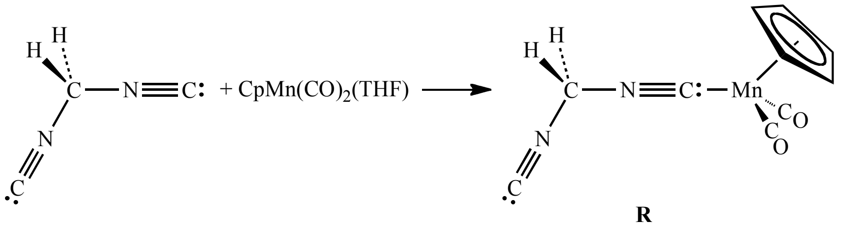

R

13.56 There are 0.00300 mmol of dimers in the solution. Of the metals in these dimers, one third are Mo and two thirds are W.

The probability that a particular molecule has the formula $[CpMo(CO)_3]_2$ = 1/3 × 1/3 = 1/9. Therefore, 1/9 × total moles = 1/9 × 0.00300 mmol = 0.00033 mmol $[CpMo(CO)_3]_2$.

The probability that a molecule has the formula $[CpW(CO)_3]_2$ = 2/3 × 2/3 = 4/9, and 4/9 × 0.00300 mmol = 0.00133 mmol $[CpW(CO)_3]_2$.

The probability that a molecule has the formula $Cp(CO)_3Mo–W(CO)_3Cp$ = 2 × 1/3 × 2/3 = 4/9, and 4/9 × 0.00300 mmol = 0.00133 mmol $Cp(CO)_3Mo–W(CO)_3Cp$.

13.57 The IR bands at 1945 and 1811 cm^{-1} are similar to those of $[Ti(CO)_4(\eta^5\text{-}C_5H_5)]^-$, suggesting similarites in structure and charge between this Ti complex and **Z**. If the other IR bands are for B–H stretches and the ^1H NMR shows two signals of relative area 3:1, it is reasonable to suggest that the boron might be present in the BH_4^- ion, with three of the hydrogens in one environment, the fourth in another. The peak at 2495 cm^{-1} is distinctly different in energy from the peaks at 2132 and 2058 cm^{-1} and might correspond to a stretch involving the less abundant of the protons. All is consistent with a structure having four CO ligands and one BH_4^- ligand (which has replaced the cyclopentadienyl ligand), and a negative charge.

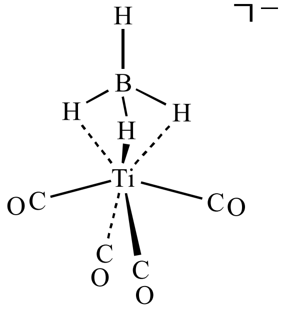

Z

Symmetry analysis indicates that this complex should have two C–O stretching bands in the infrared (A_1 and E in local C_{4v} symmetry) and three B–H bands (two A_1 and one E in local C_{3v} symmetry). The higher energy B–H stretch is for the terminal H; the lower energy bands are for the bridging H atoms.

13.58 Elemental analysis: calculated: 36.4% C, 6.10% H by mass. ^1H NMR: peak at δ 2.02 corresponds to methyl groups on Cp ring (15 protons), peak at δ –11.00 corresponds to hydrides (which typically have negative chemical shifts) (5 protons); protons are in desired 3:1 ratio. IR: If the environment around the osmium is assigned C_{4v} symmetry, using the method of Chapter 4 gives the representation:

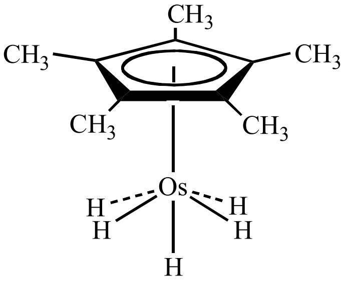

C_{4v}	E	$2C_4$	C_2	$2\sigma_v$	$2\sigma_d$
Γ	5	1	1	3	1

This reduces to $2A_1 + B_1 + E$. The A_1 and E representations are IR-active, for a total of three IR-active vibrational modes, matching the three bands in the spectrum.

13.59 **a.**

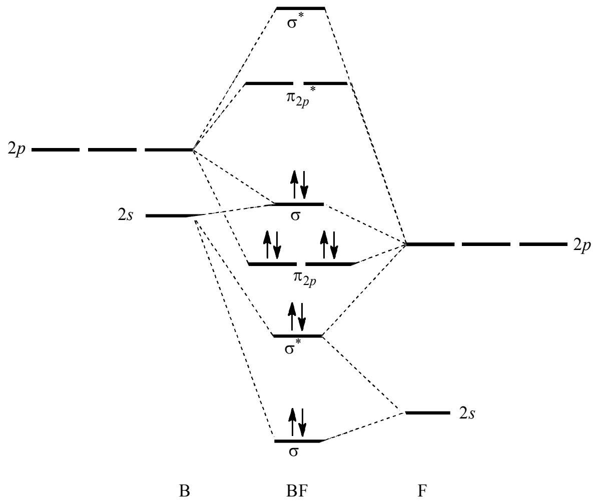

b. Because the π* orbitals of BF are concentrated on the boron to an even greater extent than π* orbitals of CO are concentrated on the carbon (because the difference in electronegativity between the atoms in BF is greater than the difference in electronegativity between the atoms in CO), BF would be expected to be a stronger π-acceptor ligand. (For a computational comparison of BF, CO, and other diatomic ligands, see U. Radius, F. M. Bickelhaupt, A. W. Ehlers, N. Goldberg, and R. Hoffmann, *Inorg. Chem.* **1998**, *37*, 1080.)

c. The stronger π-acceptor nature of BF should reduce the concentration of electrons on the Ru atoms in comparison with $[(\eta^5\text{-}C_5H_5)Ru(CO)_2]_2$. Consequently, the carbonyl ligands in the BF complex would not act as strongly as π-acceptors, and the C–O stretching vibrations should be at higher energies than 1939 and 1971 cm^{-1} (reported values are 1960 and 2012 cm^{-1}).

13.60 The product is hexaferrocenylbenzene (Figure 13.32)! In addition to being inherently interesting because of its structure and symmetry, it has potential as a precursor to a variety of derivatives whose properties could be tunable for electronic, catalytic, and other applications. The article provides references to these and other potential applications.

13.61

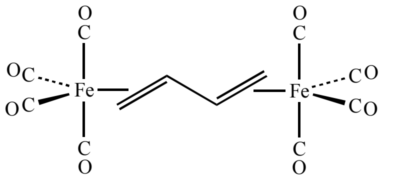

Spectral data are interpreted in the reference.

13.62 Different software and different parameter settings will generate orbitals with slightly different shapes and energies than those shown in the text, although the results should be similar. The relative energies in Part *c* in particular may differ from those in the text, because this calculation is sensitive to the methods used. In Part *d* the d_{z^2} conical nodal surface of the orbital is close to the *p* orbitals of the C_5H_5 rings (the d_{z^2} lobes point toward the centers of the rings), so the interaction between this orbital and the rings is weak.

13.63 Two orbitals that show ethylene as both a donor and acceptor are shown below.

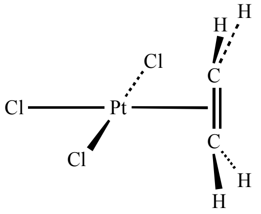

Donor interaction (from π orbital of ethylene):

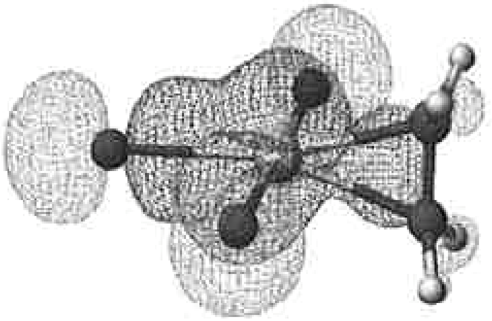

Acceptor interaction (involving π* orbital of ethylene):

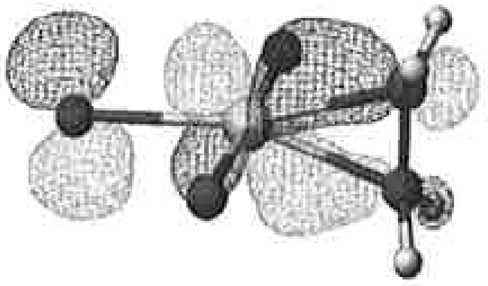

13.64 The shapes of the orbitals should be similar to those in Figure 13.8. The e_g* orbitals have different shapes because the *d* orbitals involved (d_{z^2} and $d_{x^2-y^2}$) have different shapes.

13.65 **a.** See orbitals in Section 13.4.4, page 499.

b.

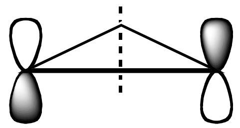

p_x, d_{xz}

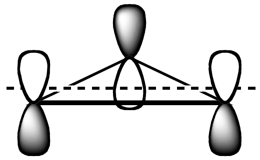

p_y, d_{yz}

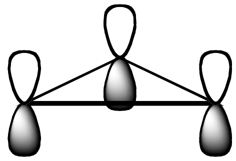

s, p_z, d_{z^2}

c. Depending on the parameters used, the upper and lower lobes of the *p* orbitals should merge in the lowest energy π orbital (to give clouds above and below the plane of the nuclei), and the lobes of two *p* orbitals in one of the upper π orbitals (derived from the *p* orbitals in front in the diagram at upper right, above) may also merge.

d. The analysis can proceed similarly to the discussion of ferrocene in Section 13.5.2.

13.66 a.

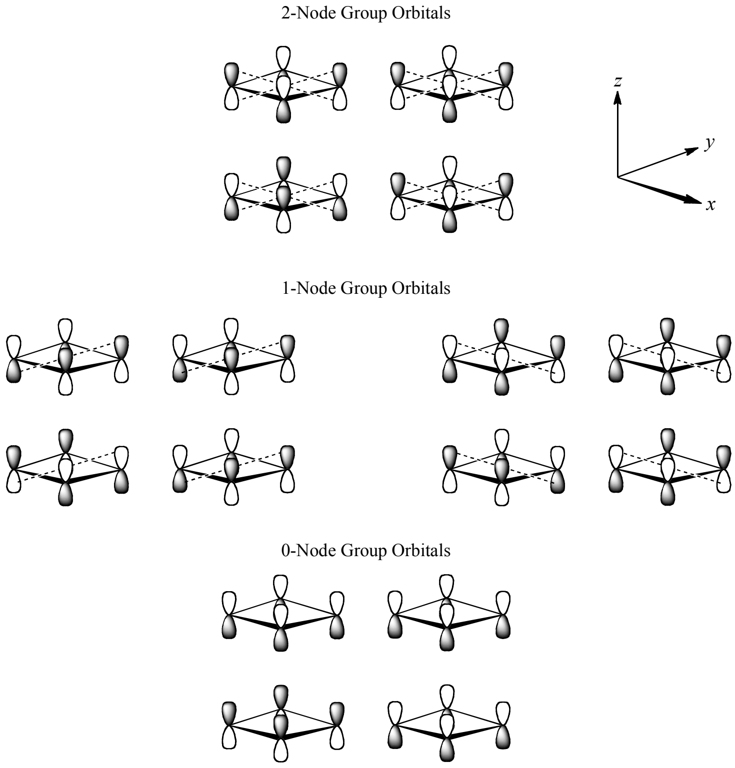

b.

2-Node Group Orbitals:		d_{xy}	none	
1-Node Group Orbitals:	p_x	d_{xz}	p_y	d_{yz}
0-Node Group Orbitals:		s, d_{z^2}	p_z	

c. The representation Γ, shown below, reduces to the irreducible representations listed. These match the group orbitals and their matching metal orbital assignments in Parts *a* and *b*. The valence *s* orbital matches the A_{1g} representation, so both the *s* and d_{z^2} orbitals of nickel can interact with the zero-node group orbital on the left.

D_{4h}	E	$2C_4$	C_2	$2C_2'$	$2C_2''$	i	$2S_4$	σ_h	$2\sigma_v$	$2\sigma_d$	
Γ	8	0	0	0	0	0	0	0	0	4	
A_{1g}	1	1	1	1	1	1	1	1	1	1	z^2
B_{2g}	1	–1	1	–1	1	1	–1	1	–1	1	xy
A_{2u}	1	1	1	–1	–1	–1	–1	–1	1	1	z
B_{1u}	1	–1	1	1	–1	–1	1	–1	–1	1	
E_g	2	0	–2	0	0	2	0	–2	0	0	(xz, yz)
E_u	2	0	–2	0	0	–2	0	2	0	0	(x, y)

d. Comparisons can be made similarly to those for ferrocene in Section 13.5.2.